Concerted measurements of lipid classes in seawater and on submicron aerosol particles at the Cape Verde Islands: biogenic sources, selective transfer and high enrichments

Nadja Triesch[1], Manuela van Pinxteren[1], Sanja Frka[2], Christian Stolle[3,4], Tobias Spranger[1], Erik Hans Hoffmann[1], Xianda Gong[1], Heike Wex[1], Detlef Schulz-Bull[3], Blaženka Gašparović[2] and Hartmut Herrmann[1*]

[1]Leibniz-Institute for Tropospheric Research (TROPOS), Leipzig, 04318, Germany
[2] Division for Marine and Environmental Research, Rudjer Boskovic Institute, Zagreb, 100000, Croatia
[3]Leibniz-Institute for Baltic Sea Research Warnemuende (IOW), Rostock, 18119, Germany
[4]Institute for Chemistry and Biology of the Marine Environment (ICBM), Carl-von-Ossietzky University Oldenburg, Wilhelmshaven, 26382, Germany

Correspondence to: Hartmut Herrmann (herrmann@tropos.de)

Supporting Information

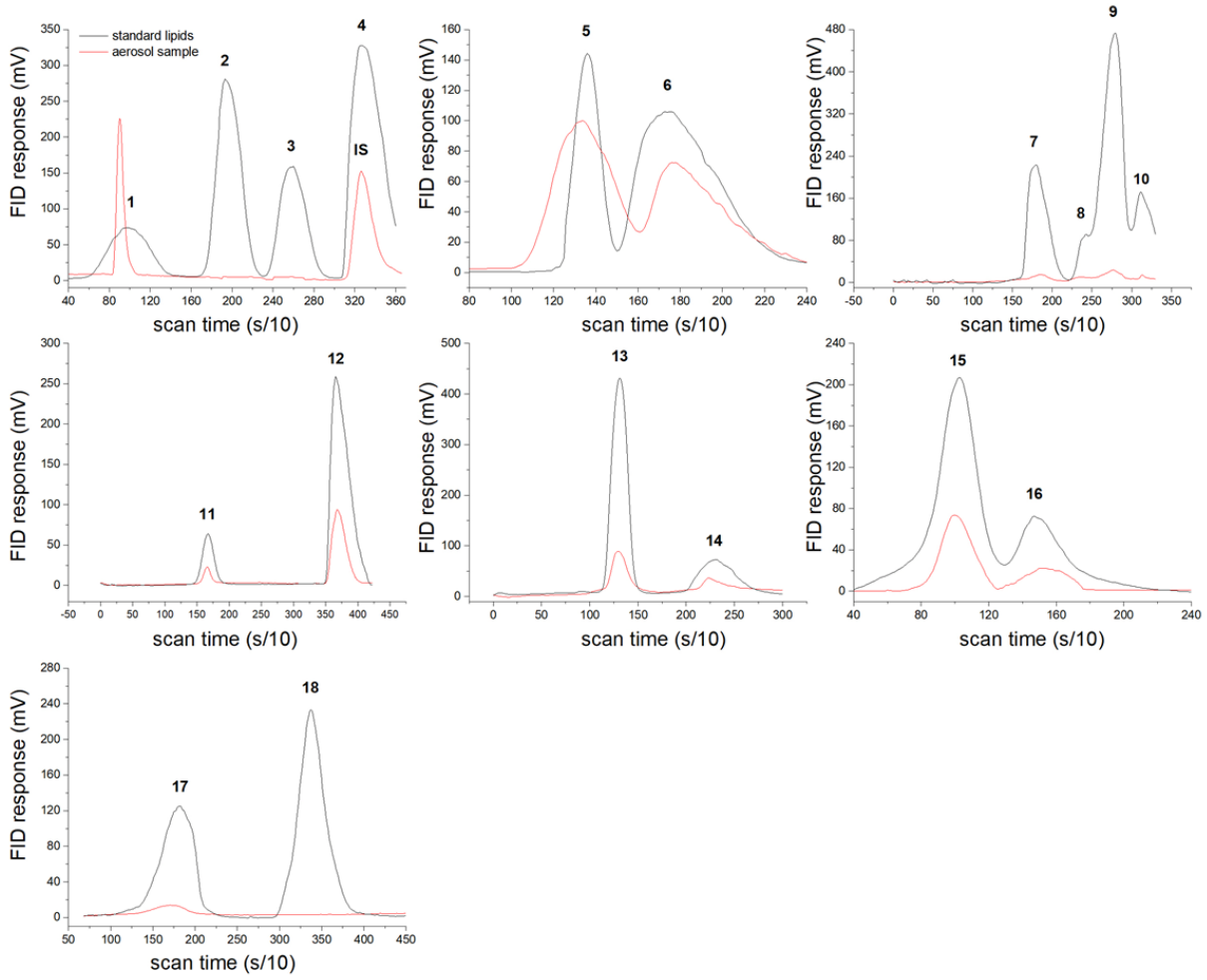

Figure S1: TLC-FID chromatogram of an aerosol sample (red) and the corresponding standards (black): lipid classes are numbered as follows: 1 HC, 2 WE, 3 ME, 4 KET (IS), 5 TG, 6 FFA, 7 ALC, 8 1,3 DG, 9 ST, 10 1.2 DG, 11 PIG, 12 MG, 13 MGDG, 14 DGDG, 15 SQDG, 16 PG, 17 PE, 18 PC

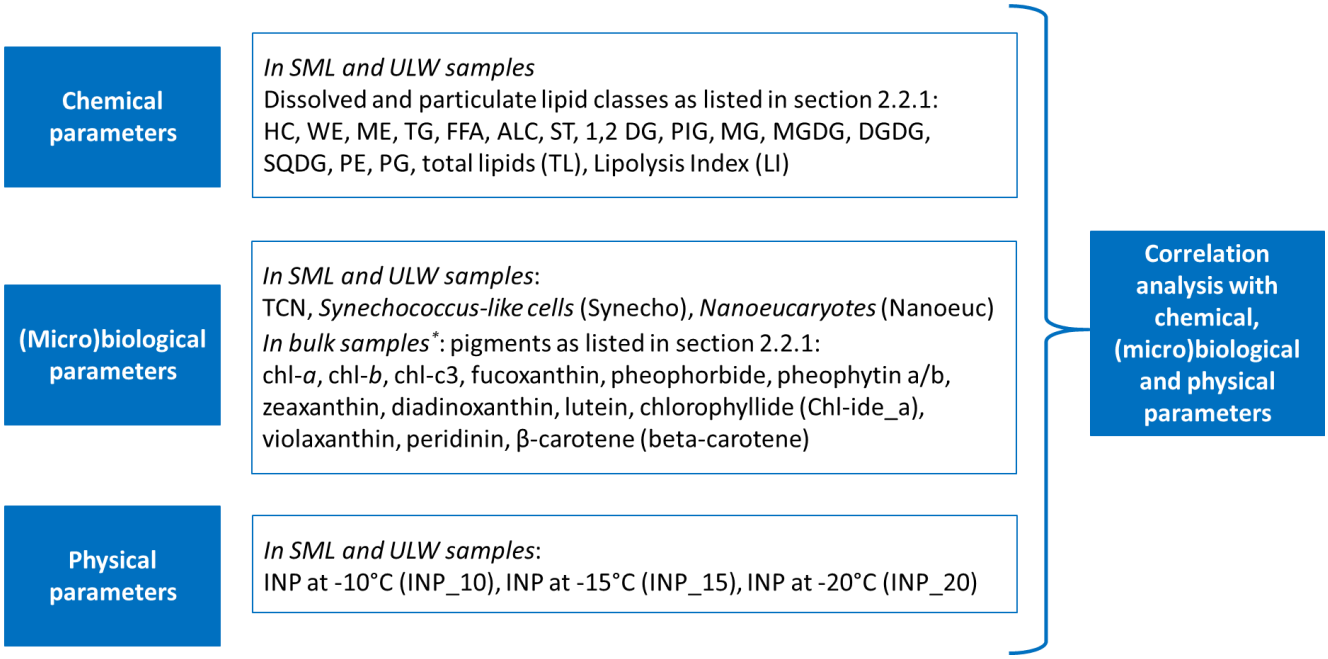

Figure S1: Overview of the chemical, (micro)biological and physical parameters and their availability in the investigated seawater samples used for the correlation analysis

* the pigments were analyzed in bulk surface water samples. These bulk surface water samples were only compared with the ULW samples in the correlation matrix. No pigment data were available for the SML samples.

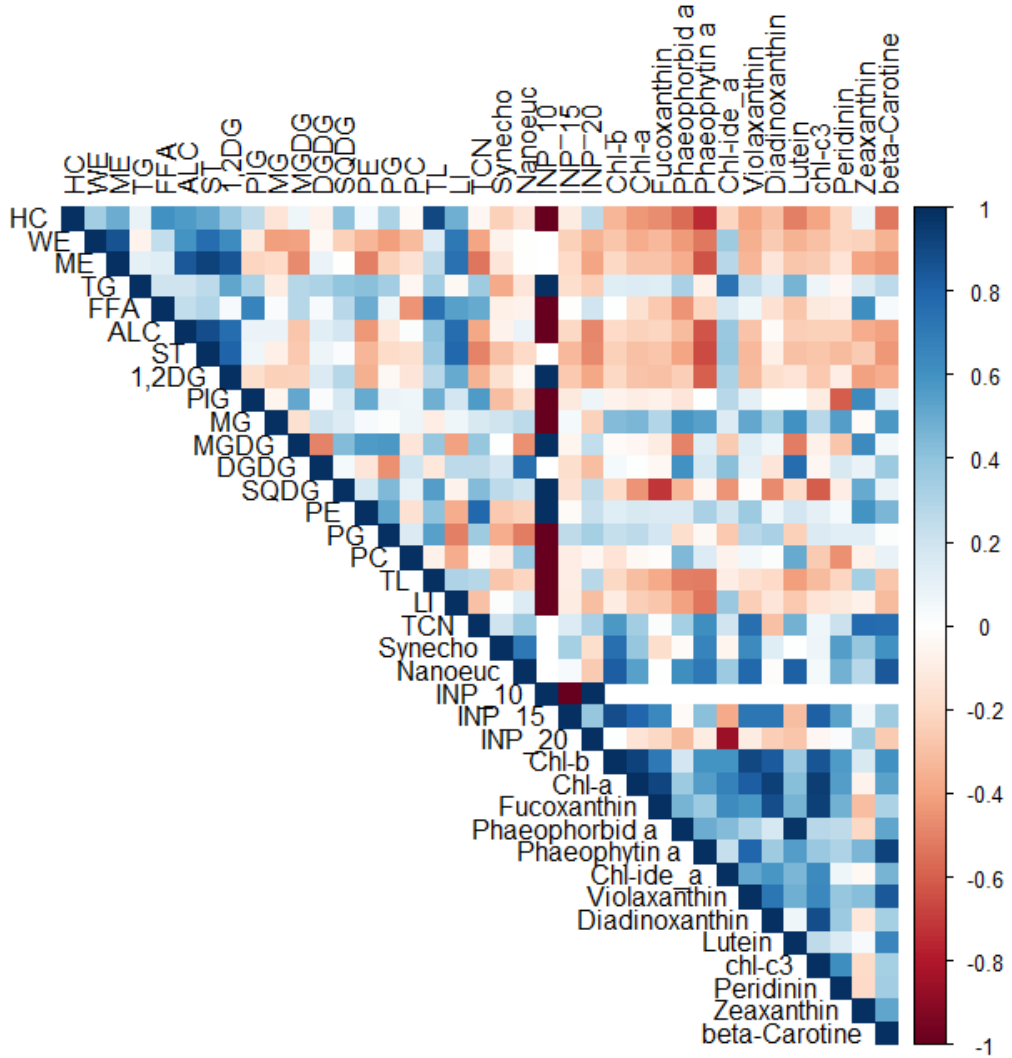

Figure S2: Statistical analysis as screening of the correlation coefficient (R) of the ULW samples focusing on the dissolved fraction of lipids; color scale of R from red (R = -1) to blue (R = 1)

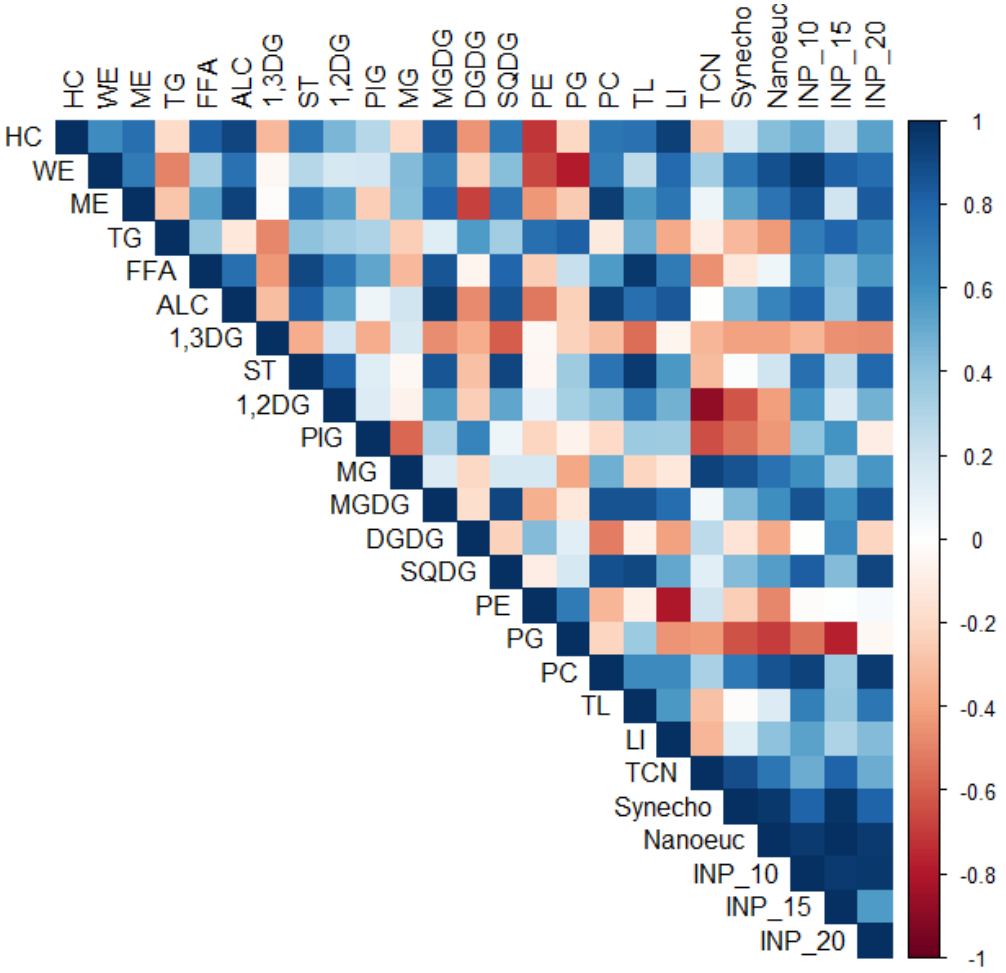

Figure S3: Statistical analysis as screening of the correlation coefficient (R) of the SML samples focusing on the dissolved fraction of lipids; color scale of R from red (R = -1) to blue (R = 1)

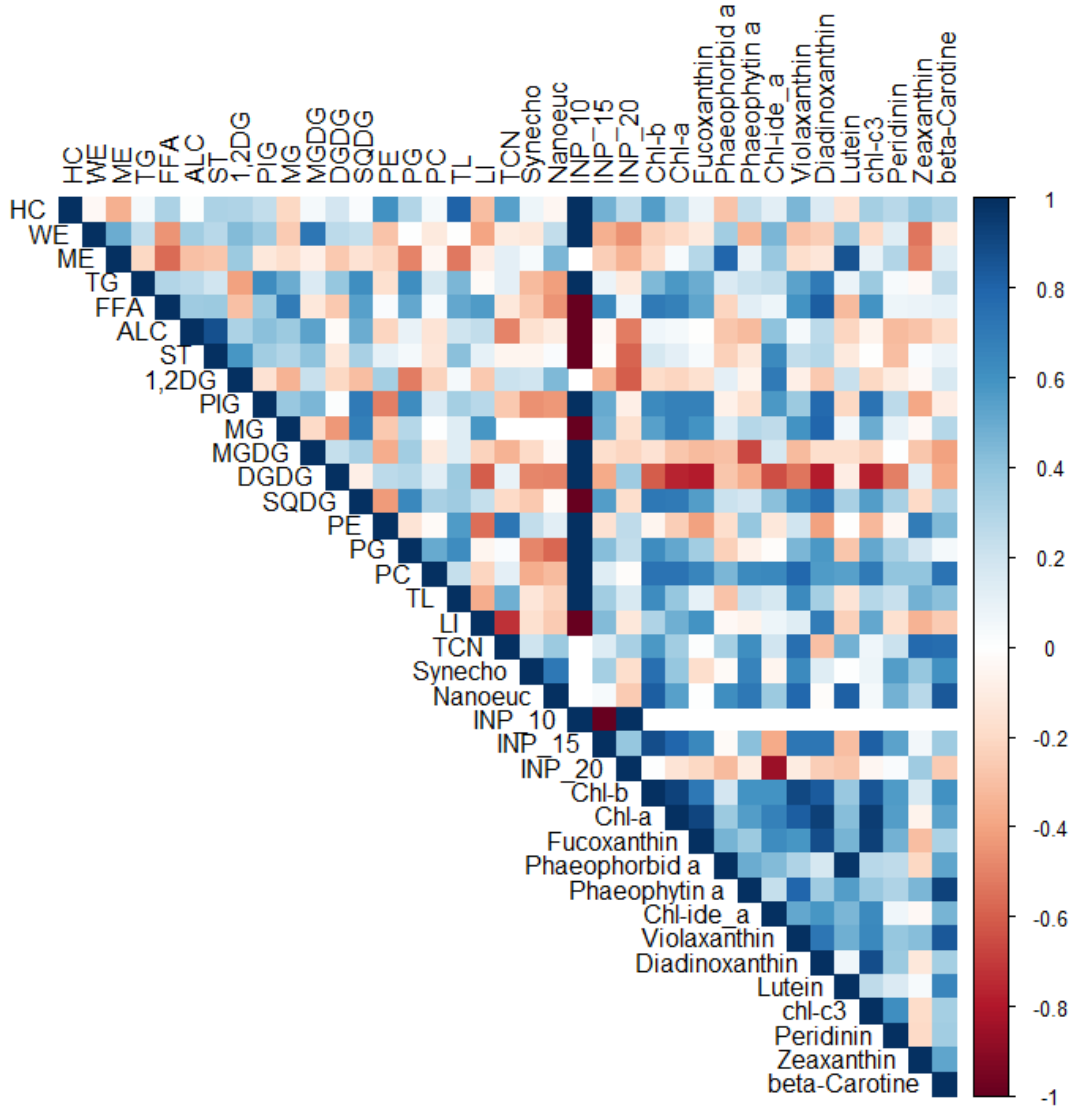

Figure S4: Statistical analysis as screening of the correlation coefficient (R) of the ULW samples focusing on the particulate fraction of lipids; color scale of R from red (R = -1) to blue (R = 1)

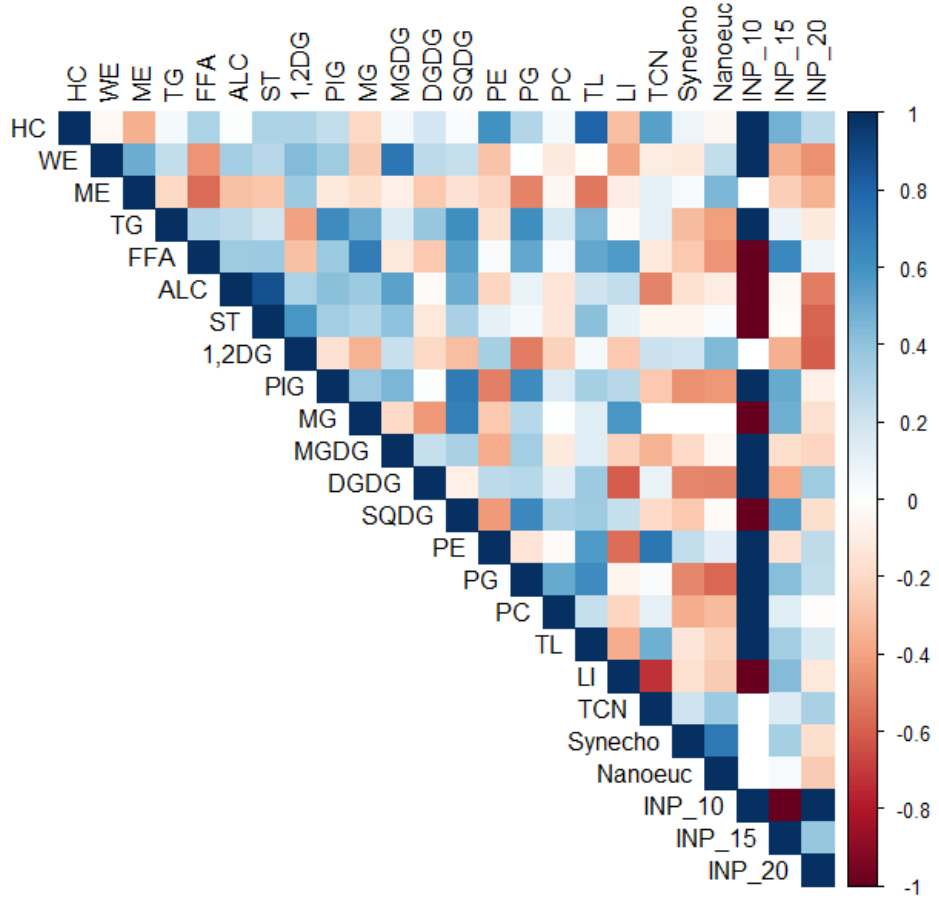

Figure S5: Statistical analysis as screening of the correlation coefficient (R) of the SML samples focusing on the particulate fraction of lipids; color scale of R from red (R = -1) to blue (R = 1)

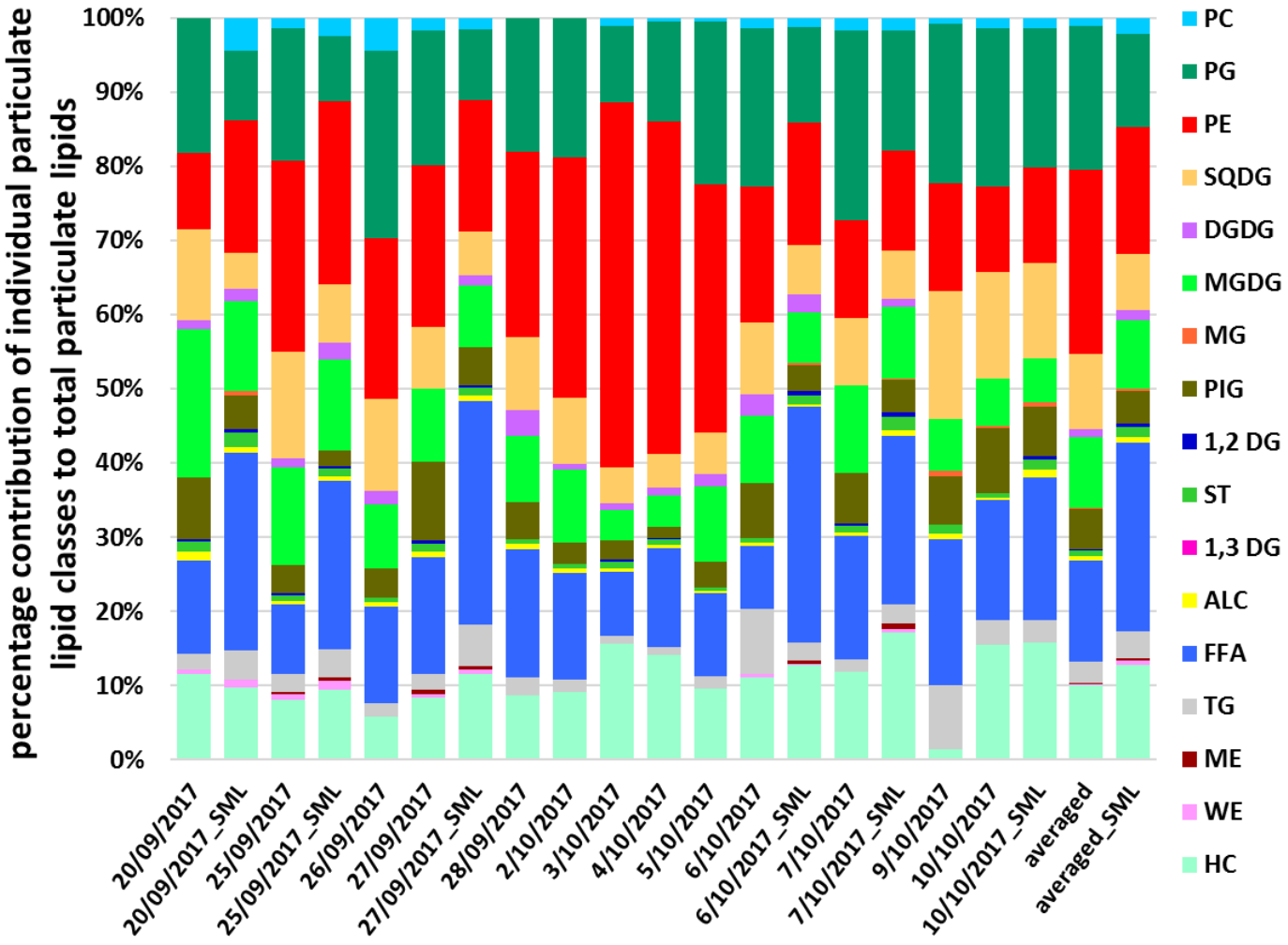

Figure S7: Percentage contribution of individual particulate lipid classes to total particulate lipids in % along the campaign and as an averaged value distinguished between ULW and SML samples

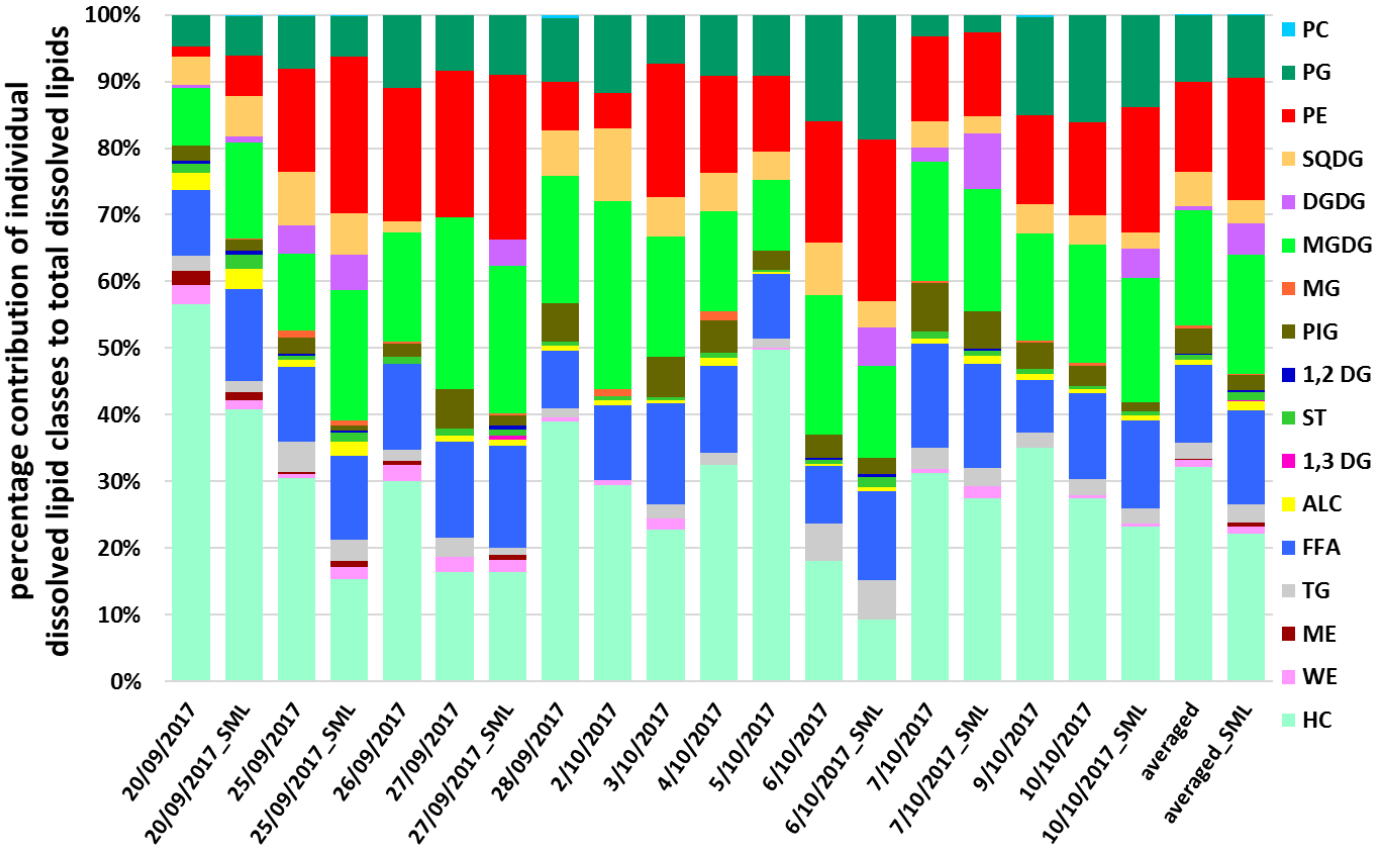

Figure S8: Percentage contribution of individual dissolved lipid classes to total dissolved lipids in % along the campaign and as an averaged value distinguished between ULW and SML samples

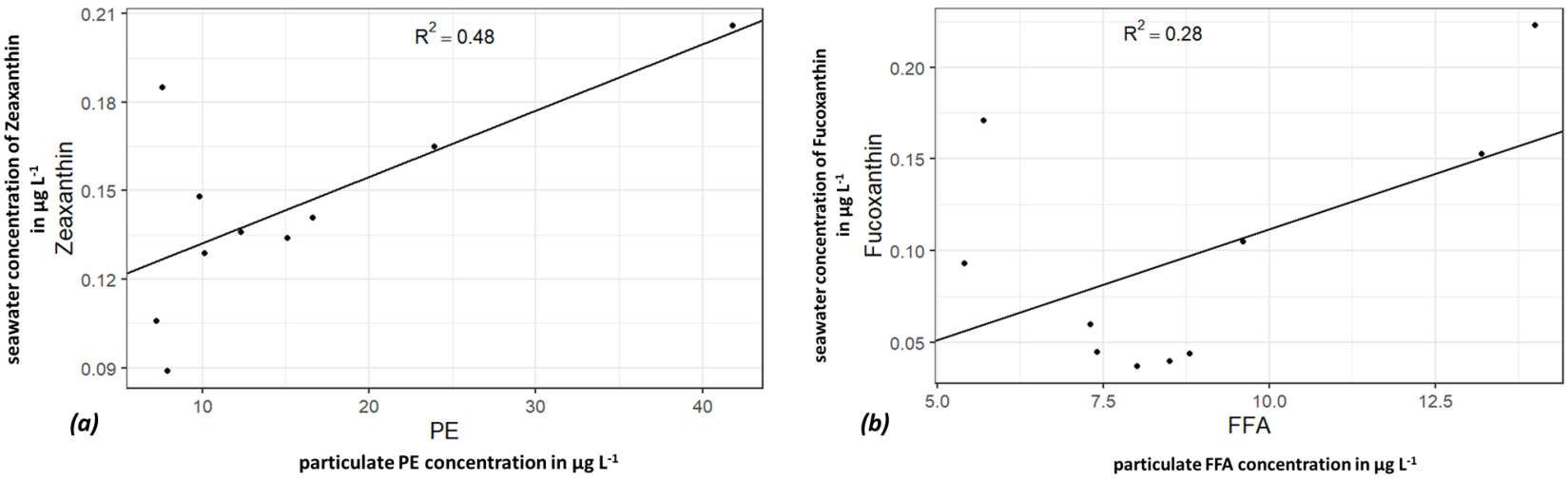

Figure S9: Correlation plot between particulate PE concentration and the concentration of (a) Zeaxanthin and (b) Fucoxanthin as proxy for autotrophic organisms in the ULW samples

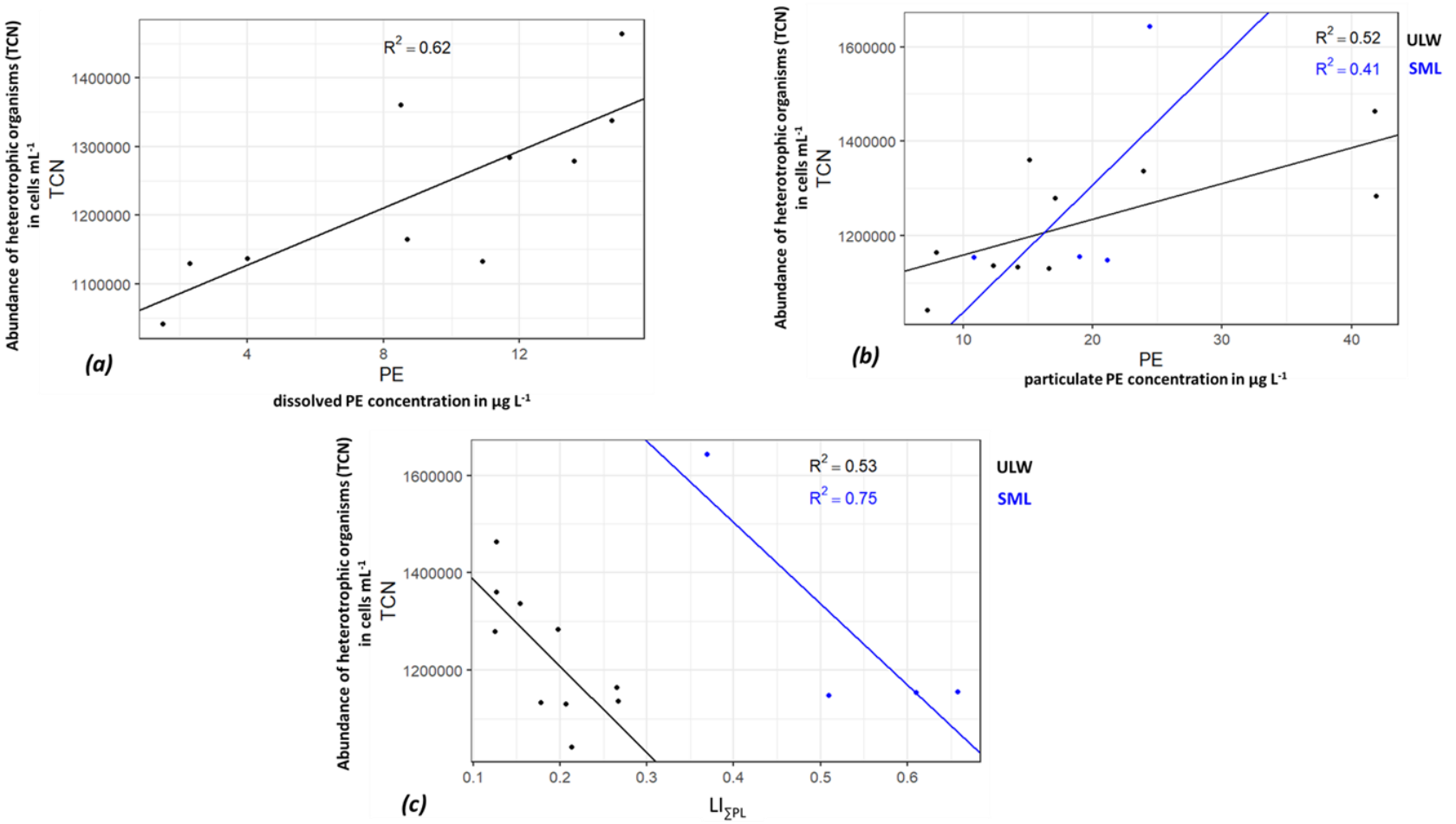

Figure S10: Correlation plot between (a) concentration of dissolved PE and TCN in ULW samples, between (b) concentration of particulate PE and TCN ULW (black) and SML (blue) samples and between (c) Lipolysis index of total particulate lipids ($LI_{\sum PL}$) and TCN concentration in ULW (black) and SML (blue) samples

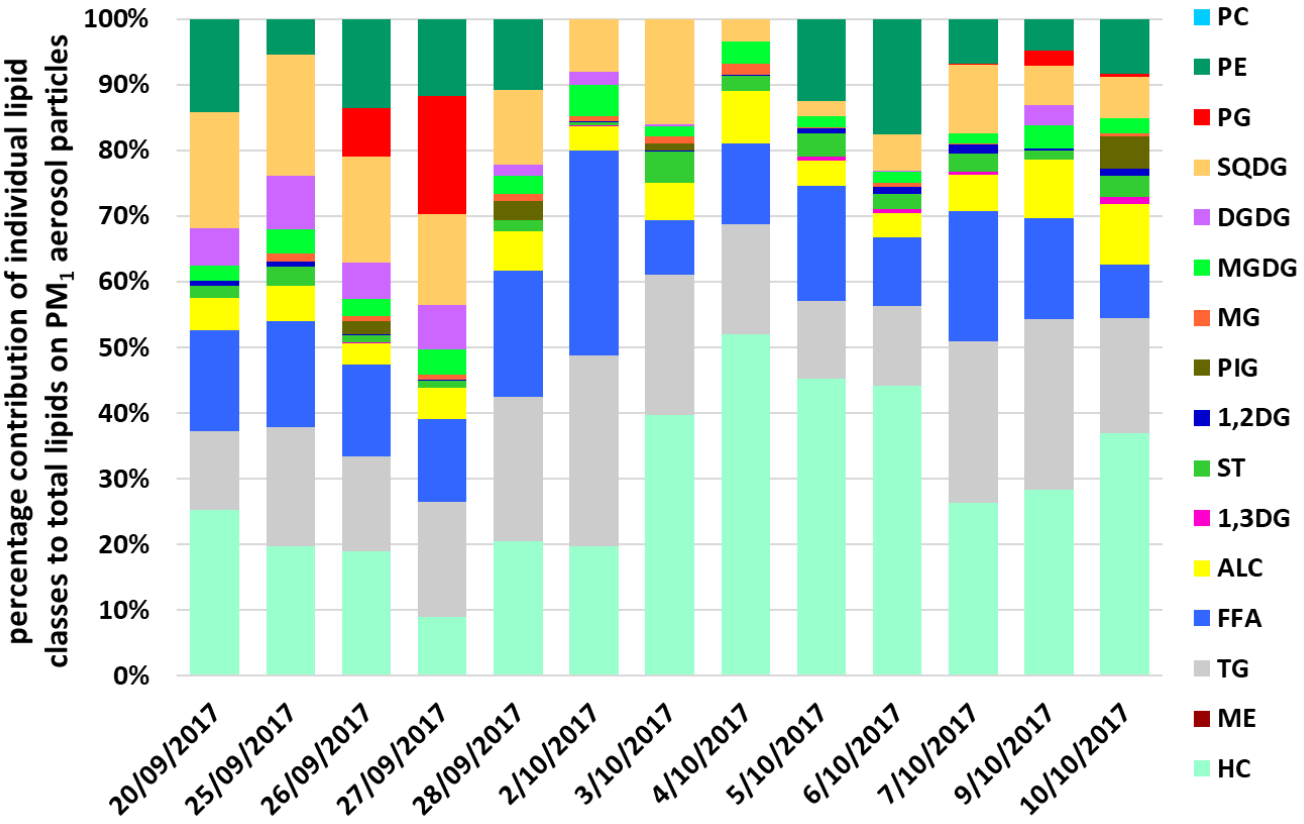

Figure S11: Percentage contribution of individual dissolved lipid classes to total lipids in % on the PM_1 aerosol particles at the CVAO along the campaign

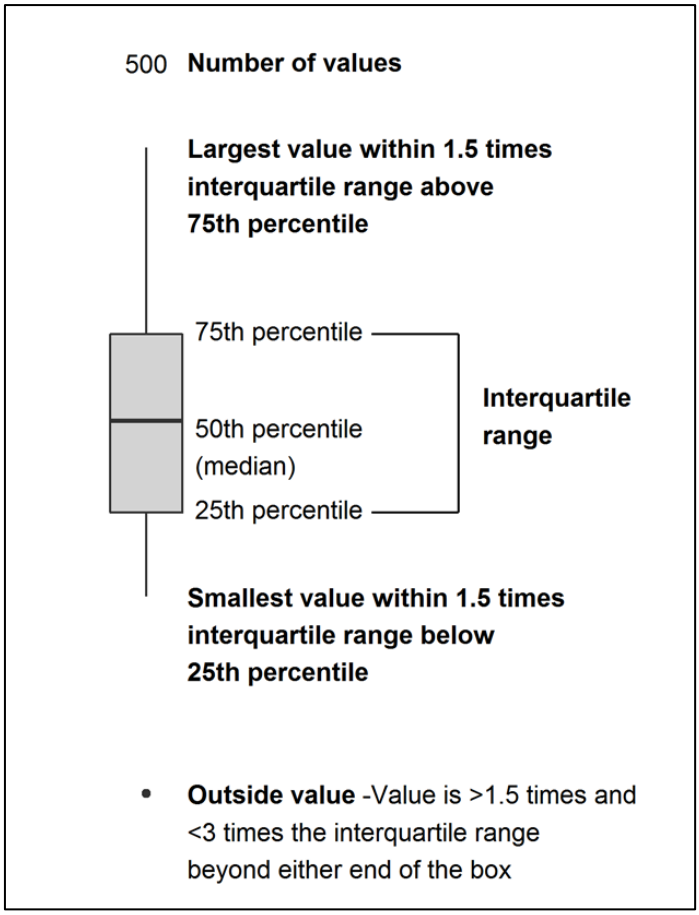

Figure S12: Boxplot explanation related to Fig. 4

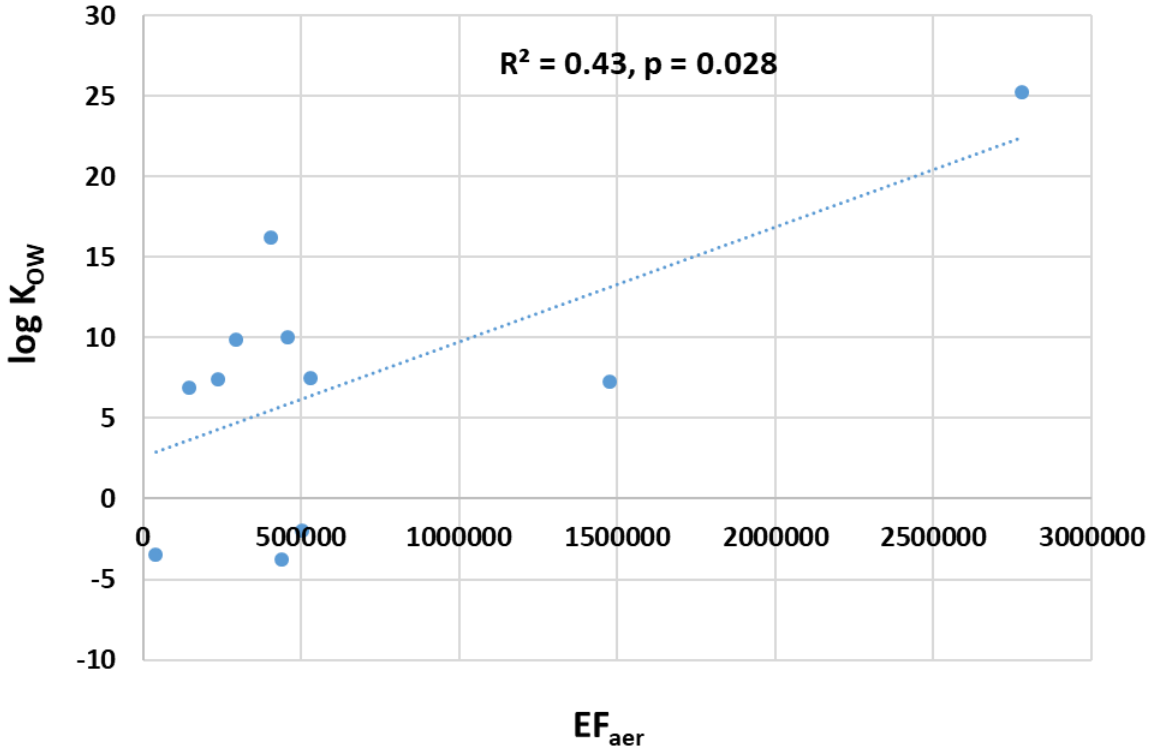

Figure S13: Correlation plot of the EF_{aer} and the corresponding log K_{OW} of the individual lipid classes: HC, TG, FFA, ALC, ST, 1,2DG, MGDG, DGDG, SQDG, PG, PE

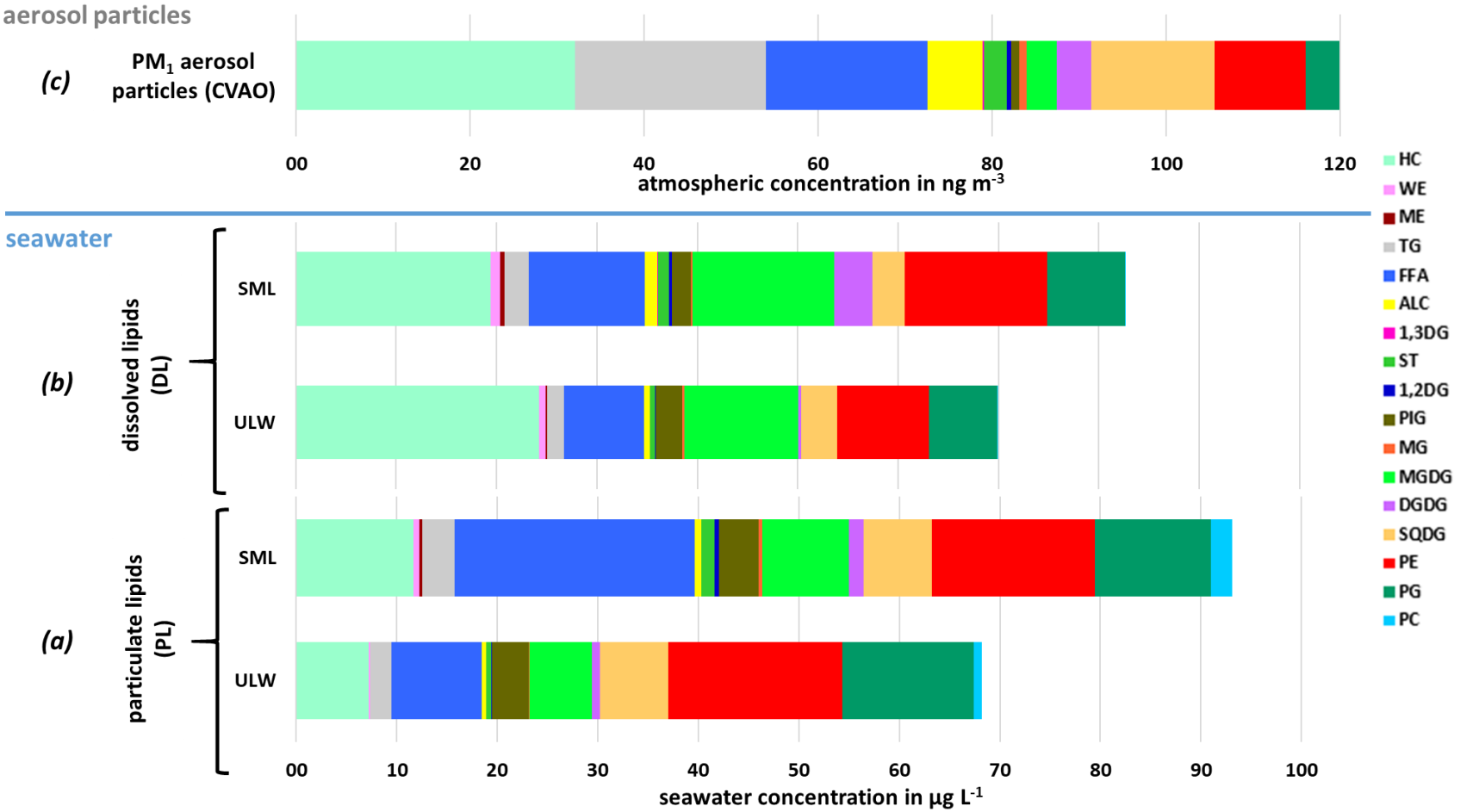

Figure S14: Concerted measurements of individual lipid classes in the (a) particulate and (b) dissolved fraction in seawater (differentiation between ULW and SML) and on (c) PM_1 aerosol particles at the CVAO; the lipid concentrations in seawater are in µg L^{-1} and on aerosol particles as atmospheric concentration in ng m^{-3}

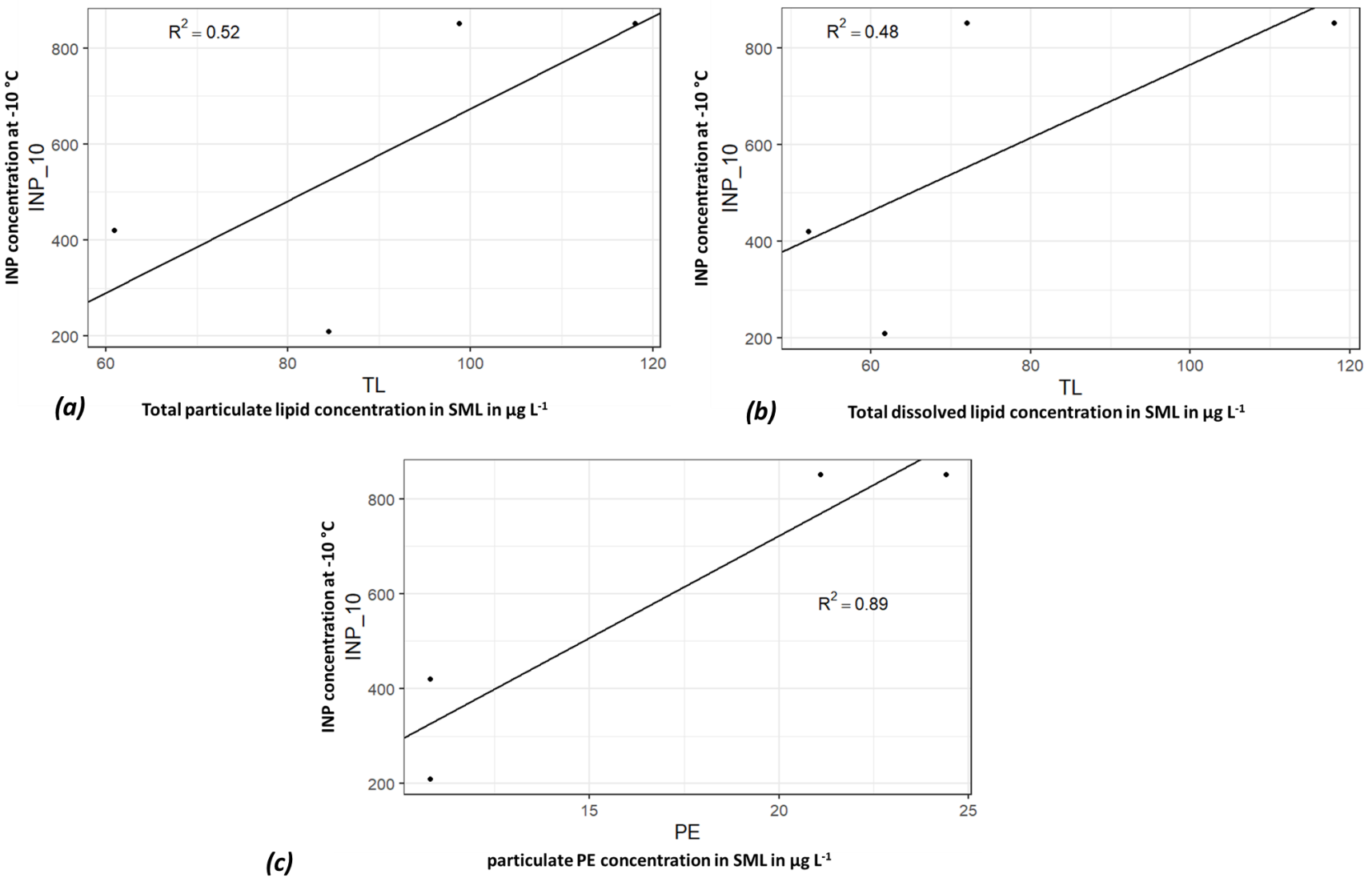

Figure S15: Correlation plot between (a) concentration of total particulate lipids and INP at -10 °C in SML samples, between (b) concentration of total dissolved lipids and INP at -10 °C in SML samples and between (c) concentration of particulate PE and INP at -10 °C in SML samples

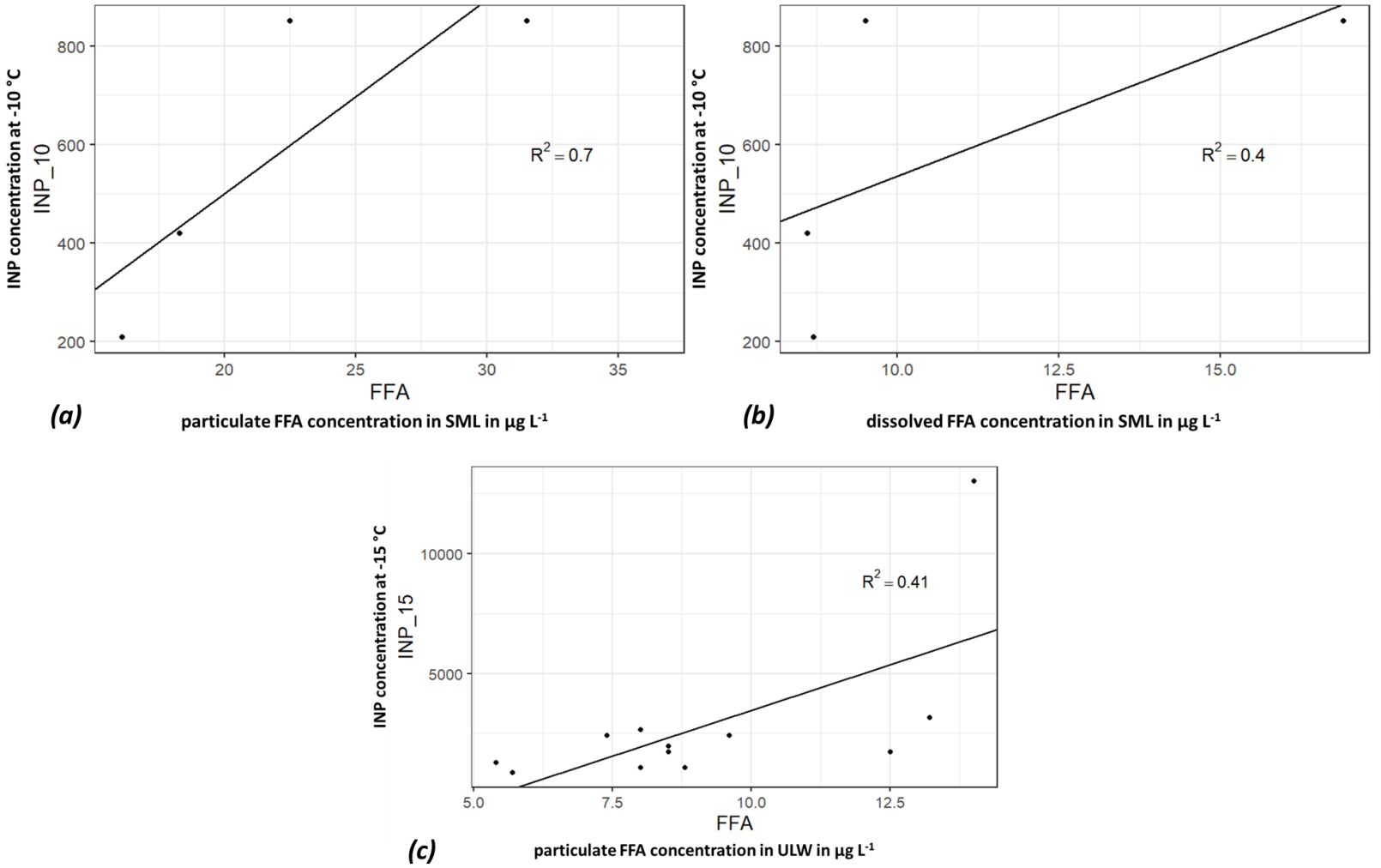

Figure S16: Correlation plot between (a) concentration of particulate FFA and INP at -10 °C in SML samples, between (b) concentration of dissolved FFA and INP at -10 °C in SML samples and between (c) concentration of particulate FFA and INP at -15 °C in ULW samples

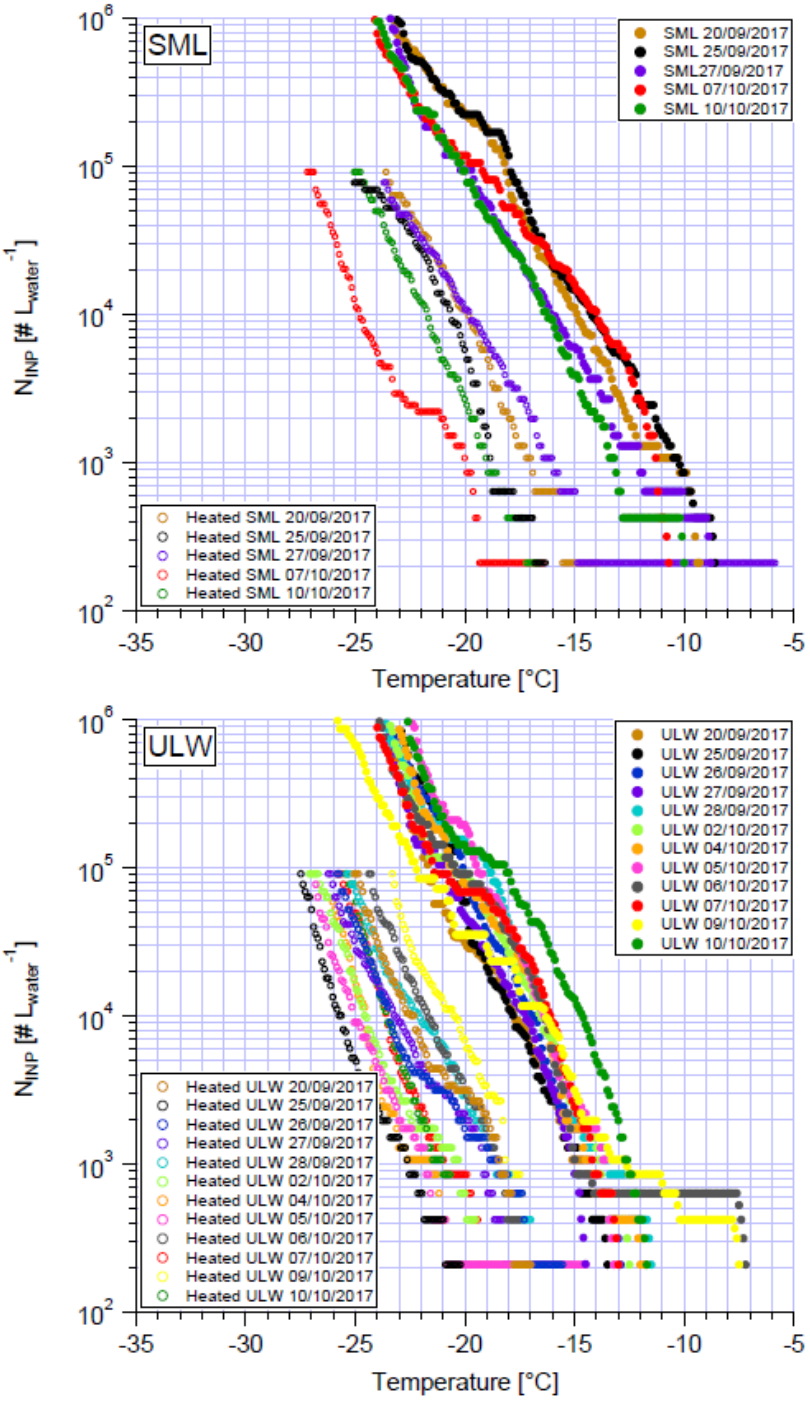

Figure S17: number of active INP in seawater distinguished between SML (above) and ULW (below) for non-heated and heated (95 °C) samples

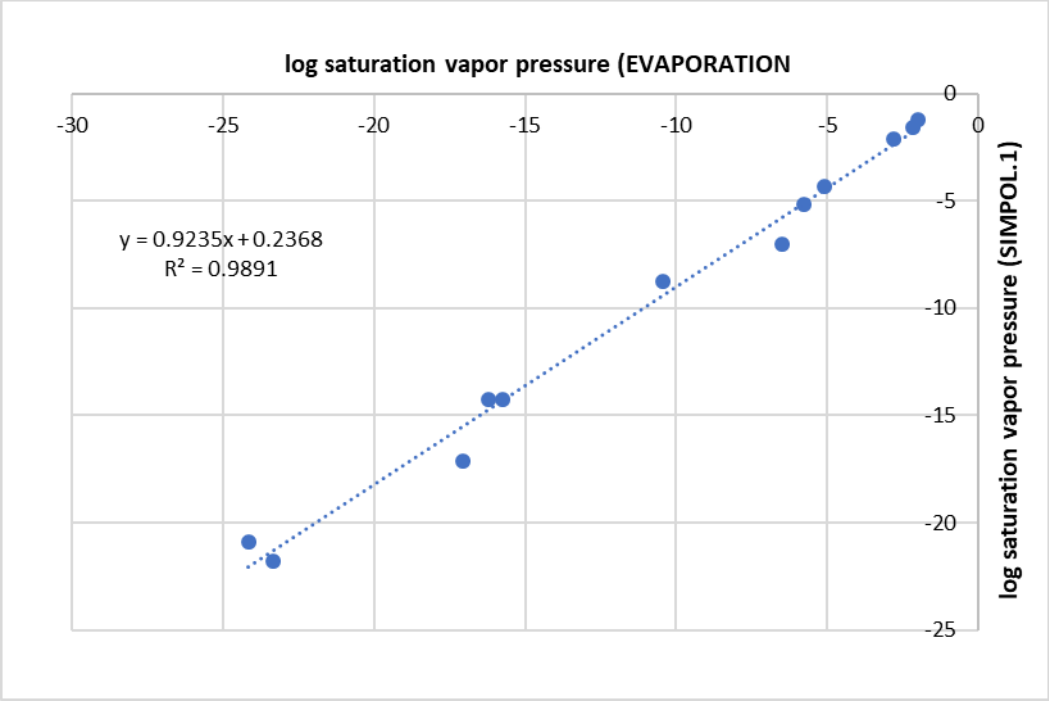

Figure S18: Comparison of the saturation vapor pressure (p) of the individual standards calculated with EVAPORATION (x-axis) and with SIMPOL.1 (y-axis); values displayed as log values

In addition to SIMPOL.1 (Pankow and Asher, 2008), the EVAPORATION model (Compernolle et al., 2011) was used to calculate the saturation vapor pressure (p) for comparison (Fig. S17). Comparing both calculation methods (Fig. S18) of p, SIMPOL.1 and EVAPORATION, showed that their values for the saturation vapor pressure of the individual standards as representatives of the lipid classes were in good agreement (R^2=0.989).

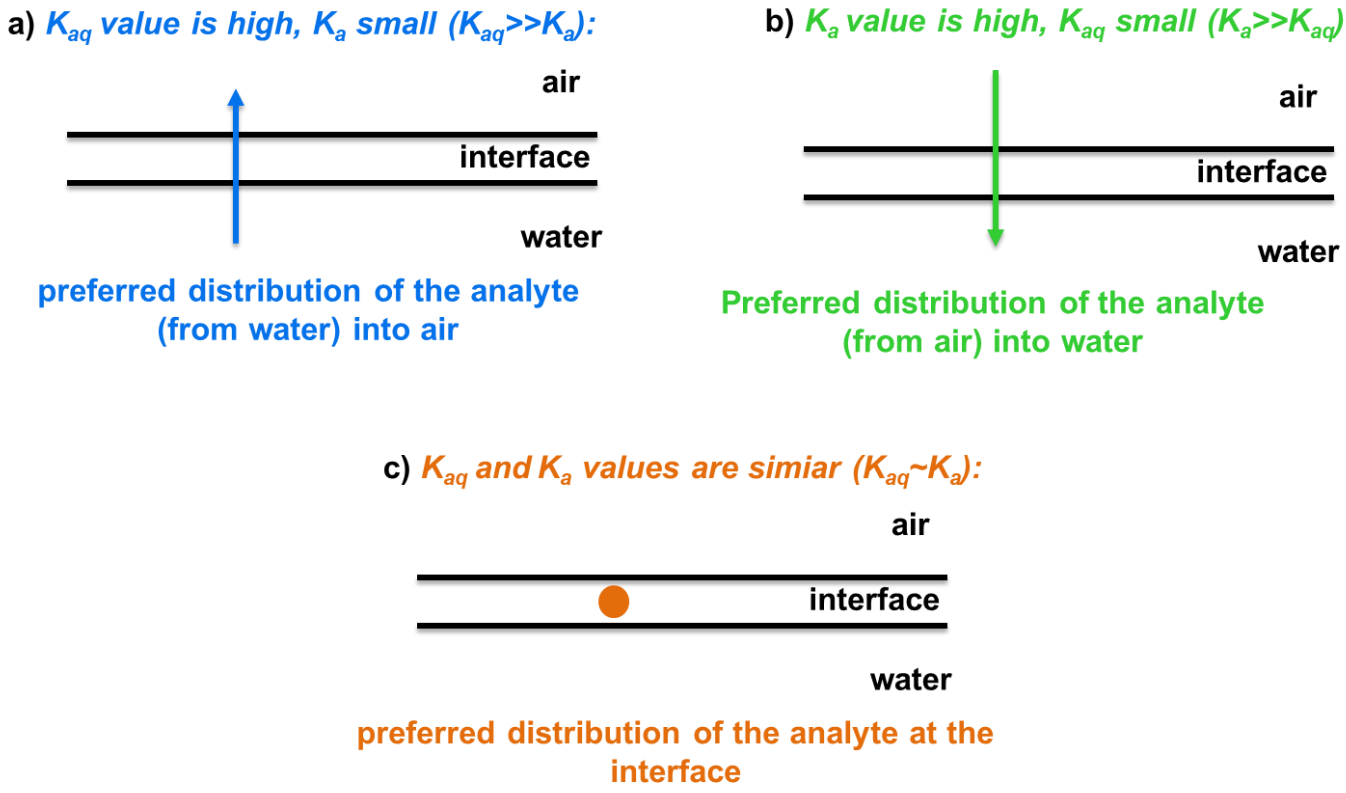

Figure S19: Overview of possible distributions of the analyte between interface, water and air: a) K_{aq}>>K_a, analyte is preferred distributed (from water) to air; b) K_a>>K_{aq}, analyte is preferred distributed (from air) into water; c) K_{aq}~ K_a, analyte is preferred distributed at the interface

Table S1: Investigated nutrients during the campaign in the ULW and the SML samples and as an averaged value in µmol L^{-1}; dinitrogen trioxide (N_2O_3), nitrogen dioxide (NO_2), nitrate (NO_3^-), phosphate (PO_4^{3-}) and silicates (SiO_4^{4-}); LOQ: limit of quantification; NA: not available

Sampling date	µmol L^{-1}									
	N_2O_3		NO_2		NO_3^-		PO_4^{3-}		SiO_4^{4-}	
	ULW	SML	ULW	SML	ULW	SML	ULW	SML	ULW	SML
20/09/2017	0.36	0.50	< LOQ	0.02	0.36	0.49	0.09	0.19	0.60	1.25
25/09/2017	0.28	0.66	0.01	0.02	0.28	0.64	0.06	0.15	1.00	1.40
26/09/2017	0.52	0.47	0.03	0.03	0.49	0.44	0.05	0.08	1.00	1.40
27/09/2017	0.24	0.32	0.02	0.01	0.22	0.31	0.12	0.07	2.20	1.20
28/09/2017	0.25	0.38	0.00	0.03	0.25	0.35	0.07	0.13	1.10	0.90
2/10/2017	0.91	NA	0.03	NA	0.89	NA	0.07	NA	1.90	NA
3/10/2017	0.22	NA	0.01	NA	0.21	NA	0.10	NA	1.45	NA
4/10/2017	0.31	NA	0.01	NA	0.30	NA	0.10	NA	0.50	NA
5/10/2017	0.35	NA	0.02	NA	0.33	NA	0.09	NA	1.00	NA
6/10/2017	0.18	0.23	0.03	0.03	0.16	0.20	0.06	0.02	0.50	0.50
7/10/2017	0.28	0.26	0.07	0.04	0.22	0.22	0.23	0.04	0.35	0.10
averaged	0.35	0.40	0.02	0.02	0.33	0.38	0.09	0.09	1.05	0.96

Table S2: Pigment concentration in the bulk surface water in µg L^{-1} along the campaign in 2017; * investigated pigment was not measured

pigments	18/09	20/09	25/09	27/09	28/09	02/10	03/10	05/10	07/10	09/10	10/10
chlorophyll c2	1.63E-02	2.56E-02	3.05E-02	4.13E-02	2.30E-02	2.88E-02	2.81E-02	2.46E-02	3.85E-02	3.88E-02	6.16E-02
19-butyl fucoxanthin	4.79E-04	1.75E-02	1.94E-03	1.80E-02	4.01E-03	1.85E-02	1.24E-02	1.32E-02	2.57E-02	3.11E-02	5.79E-02
19-hexanoyl fucoxanthin	1.46E-02	4.41E-02	1.81E-02	4.53E-02	2.70E-02	4.48E-02	3.32E-02	3.10E-02	6.25E-02	6.87E-02	1.10E-01
chlorophyll-*b*	2.10E-02	4.22E-02	5.48E-02	3.81E-02	3.18E-02	5.00E-02	6.15E-02	3.50E-02	6.27E-02	6.53E-02	1.09E-01
chlorophyll-*a*	1.12E-01	2.16E-01	3.23E-01	3.35E-01	1.84E-01	2.64E-01	2.98E-01	1.92E-01	3.46E-01	4.37E-01	6.04E-01
fucoxanthin	1.45E-02	4.37E-02	9.35E-02	1.71E-01	3.97E-02	4.54E-02	6.04E-02	3.68E-02	1.05E-01	1.53E-01	2.23E-01
pheophorbide a	3.13E-02	3.23E-02	4.70E-02	4.13E-02	3.73E-02	3.37E-02	3.57E-02	3.27E-02	3.65E-02	3.88E-02	3.79E-02
pheophytin a	1.71E-02	1.78E-02	2.69E-02	2.28E-02	2.29E-02	2.64E-02	2.92E-02	2.05E-02	2.51E-02	2.64E-02	2.74E-02
chlorophyllide a	0.00E+00	1.00E-02	1.00E-02	1.00E-02	0.00E+00	0.00E+00	1.00E-02	0.00E+00	1.00E-02	1.00E-02	*
violaxanthin	*	3.49E-03	4.67E-03	3.08E-03	2.60E-03	4.29E-03	5.54E-03	3.19E-03	5.36E-03	6.40E-03	7.03E-03
diadinoxanthin	9.16E-03	1.81E-02	1.63E-02	2.07E-02	1.44E-02	1.74E-02	1.75E-02	1.25E-02	2.31E-02	2.99E-02	3.41E-02
lutein	1.38E-03	1.83E-03	5.09E-03	*	2.78E-03	1.85E-03	2.75E-03	1.90E-03	2.78E-03	3.33E-03	*
chlorophyll c3	1.40E-02	2.20E-02	2.66E-02	3.80E-02	1.72E-02	2.53E-02	2.49E-02	2.15E-02	3.52E-02	3.42E-02	5.93E-02
peridinin	2.62E-03	4.69E-03	7.31E-03	5.92E-03	2.75E-03	6.50E-03	4.80E-03	6.48E-03	5.16E-03	4.83E-03	7.69E-03
zeaxanthin	1.08E-01	1.06E-01	1.34E-01	8.91E-02	1.36E-01	1.41E-01	2.06E-01	1.65E-01	1.85E-01	1.48E-01	1.29E-01
ß-carotene	6.19E-03	8.72E-03	1.70E-02	1.05E-02	1.02E-02	1.33E-02	1.81E-02	1.00E-02	1.41E-02	1.46E-02	1.54E-02

Table S3: Abundances of autotrophic organisms (*Nanoeucaryotes* and *Synechococcus-like cells)* and of bacteria (TCN) in cells mL^{-1} in the ULW and the SML samples and the calculated EF_{SML} (Eq. 2) along the campaign; NA – not available

	Synechococcus-like cells			*Nanoeucaryotes*			TCN		
	ULW	SML	EF_{SML}	ULW	SML	EF_{SML}	ULW	SML	EF_{SML}
20/09/2017	1.6E+04	2.0E+04	1.2	1.5E+03	2.6E+03	1.8	1.0E+06	1.1E+06	1.1
25/09/2017	2.6E+04	3.1E+04	1.2	3.2E+03	3.4E+03	1.1	1.4E+06	1.6E+06	1.2
26/09/2017	8.0E+03	9.7E+03	1.2	6.5E+02	8.5E+02	1.3	1.1E+06	9.9E+05	0.9
27/09/2017	1.4E+04	1.3E+04	0.9	1.1E+03	9.6E+02	0.9	1.2E+06	1.2E+06	1.0
28/09/2017	1.1E+04	1.2E+04	1.1	1.3E+03	1.2E+03	0.9	1.1E+06	1.3E+06	1.2
02/10/2017	4.5E+04	2.4E+04	0.5	2.1E+03	1.4E+03	0.7	1.1E+06	1.3E+06	1.1
03/10/2017	3.2E+04	3.6E+04	1.1	2.2E+03	1.7E+03	0.8	1.5E+06	1.4E+06	0.9
04/10/2017	1.6E+04	1.9E+04	1.1	1.2E+03	1.1E+03	0.9	1.3E+06	1.2E+06	1.0
05/10/2017	1.4E+04	NA	NA	1.1E+03	NA	NA	1.3E+06	NA	NA
06/10/2017	9.9E+03	1.1E+04	1.1	4.8E+02	3.1E+02	0.7	1.3E+06	1.2E+06	0.9
averaged	1.9E+04	1.9E+04	1.1	1.5E+03	1.5E+03	1.0	1.2E+06	1.3E+06	1.0

Pigments, nutrients and microbiological investigations in seawater

The pigment measurements of bulk surface water (Table S2) indicated temporal changes in the composition of the community with total pigment concentrations between 0.4 µg L^{-1} and 1.5 µg L^{-1} during the campaign and an increasing trend in pigment concentration towards the end of the campaign. The chl-*a* concentration in seawater increased from 0.11 µg L^{-1} to 0.60 µg L^{-1} (Table S2) and was generally low compared to other subtropical/tropical regions or worldwide (Duhamel et al., 2019). A nutrient limitation (Table S1), especially for phosphate (averaged concentration of 0.09 µmol L^{-1} in each ULW and SML) could explain the low total abundance of autotrophic organisms, which is also reflected in low chl-*a* concentrations.

Nanoeucaryotes, *Synechococcus-like cells* and TCN are presented in Table S3. The mean TCN value was $1.2 \cdot 10^6 \pm 1.3 \cdot 10^5$ cells mL^{-1} in the ULW and $1.3 \cdot 10^6 \pm 1.9 \cdot 10^5$ cells mL^{-1} in the SML samples, which is consistent with previous reports for surface water of subtropical regions (Zäncker et al., 2018). The abundance of *Synechococcus-like cells* were $1.9 \cdot 10^4 \pm 1.2 \cdot 10^4$ cells mL^{-1} (ULW), $1.9 \cdot 10^4 \pm 9.1 \cdot 10^3$ cells mL^{-1} (SML) and for *Nanoeucaryotes* $1.5 \cdot 10^3 \pm 8.2 \cdot 10^2$ cells mL^{-1} (ULW), $1.5 \cdot 10^3 \pm 9.6 \cdot 10^2$ cells mL^{-1} (SML). Duhamel et al. (2019) reported a *Synechococcus* cell abundance of 2.5-9.2·10^3 cells mL^{-1}for seawater samples (20 m depth) taken in the western subtropical Atlantic Ocean. Although comparable data

are lacking, the low cell abundances in the present study are indicative of an oligotrophic system. *Synechococcus-like cells* and *Nanoeucaryotes* showed a similar trend as chl-*a* (two slight increases, followed by depression), indicating that autotrophic organisms followed similar temporal pattern.

Table S4: PE/PG ratio of the particulate fraction in the ULW and the SML samples along the campaign; NA - not available

sampling date	PE/PG ratio	
	ULW	SML
20/09/2017	0.6	1.9
25/09/2017	1.5	2.8
26/09/2017	0.9	NA
27/09/2017	1.2	1.8
28/09/2017	1.4	NA
2/10/2017	1.7	NA
3/10/2017	4.8	NA
4/10/2017	3.3	NA
5/10/2017	1.5	NA
6/10/2017	0.9	1.3
7/10/2017	0.5	0.8
9/10/2017	0.7	NA
10/10/2017	0.5	0.7
averaged	1.3	1.4

Table S5: Lipolysis Index (LI) in the ULW and in the SML samples for the dissolved and the particulate fraction of lipids; NA: not available

sampling date	dissolved fraction		particulate fraction	
	LI_{ULW}	LI_{SML}	LI_{ULW}	LI_{SML}
20/09/2017	0.53	0.48	0.21	0.51
25/09/2017	0.26	0.24	0.13	0.37
26/09/2017	0.25	NA	0.18	NA
27/09/2017	0.25	0.28	0.27	0.61
28/09/2017	0.21	NA	0.27	NA
2/10/2017	0.23	NA	0.21	NA
3/10/2017	0.28	NA	0.13	NA
4/10/2017	0.34	NA	0.20	NA
5/10/2017	0.27	NA	0.15	NA
6/10/2017	0.13	0.20	0.12	0.66
7/10/2017	0.38	0.35	0.27	0.46
9/10/2017	0.18	NA	0.31	NA
10/10/2017	0.25	0.23	0.29	0.38
averaged	0.27	0.30	0.21	0.50

Table S6: Enrichment factor in SML (EF_{SML}) of the individual lipid classes in the particulate fraction (PF) and in the dissolved fraction (DF) along the campaign and as an average; NA - not available

Lipid classes	20/09/2017		25/09/2017		27/09/2017		06/10/2017		07/10/2017		10/10/2017		averaged	
	PF	DF	PF	DF	PF	DF	PF	DF	PF	DF	PF	DF	PF	DF
HC	1.4	0.9	2.0	0.7	2.3	1.4	1.4	0.7	2.0	1.0	1.0	1.0	1.7	0.9
WE	2.7	0.6	2.4	4.4	2.3	1.1	0.6	NA	NA	3.4	NA	1.2	1.3	1.8
ME	NA	0.7	2.8	3.5	1.3	NA	NA	NA	NA	NA	NA	NA	0.7	0.7
TG	3.2	0.9	2.5	1.0	4.4	0.5	0.3	1.5	2.3	1.0	0.9	1.1	2.3	1.0
FFA	3.6	1.8	4.2	1.5	3.2	1.5	4.6	2.1	1.9	1.1	1.1	1.2	3.1	1.5
ALC	1.1	1.5	2.2	2.8	1.7	1.3	0.9	1.8	2.1	1.6	2.5	1.4	1.7	1.7
ST	2.5	1.9	2.4	2.9	1.7	1.4	2.9	3.3	3.0	0.9	2.4	1.3	2.5	1.9
1,2 DG	1.5	1.4	2.0	1.8	1.4	NA	NA	3.0	2.9	NA	NA	NA	1.3	1.0
PIG	0.9	1.0	0.9	0.4	0.8	0.3	0.6	0.9	0.9	0.9	0.7	0.5	0.8	0.7
MG	NA	NA	NA	0.8	NA	NA	NA	NA	NA	NA	1.8	NA	0.3	0.1
MGDG	1.0	2.1	1.6	2.3	1.4	1.2	0.9	0.9	1.2	1.2	0.9	1.2	1.2	1.5
DGDG	2.5	2.8	3.2	1.7	NA	NA	1.1	NA	NA	4.3	NA	NA	1.1	1.5
SQDG	0.7	1.8	0.9	1.0	1.2	NA	0.8	0.7	1.0	0.7	0.9	0.7	0.9	0.8
PE	2.9	4.7	1.6	2.1	1.4	1.6	1.1	1.8	1.4	1.1	1.1	1.6	1.6	2.1
PG	0.9	1.6	0.8	1.1	0.9	1.5	0.7	1.6	0.9	0.9	0.9	1.0	0.8	1.3
PC	NA	NA	2.9	1.5	1.5	NA	1.2	NA	1.5	NA	1.0	NA	1.3	0.3
total lipids	1.7	1.3	1.7	1.4	1.7	1.4	1.2	1.3	1.4	1.1	1.0	1.2	1.4	1.3
PP*	1.9	2.4	1.4	1.7	1.2	1.6	0.9	1.7	1.1	1.1	0.9	1.3	1.2	1.6
GL**	0.9	2.1	1.3	1.8	1.4	1.4	0.9	1.1	1.2	1.4	0.9	1.4	1.1	1.5

PP* - Phospholipids, including PE, PG and PC. In order to determine the enrichment factor, the sum of the concentrations of the individual lipid classes (PE, PG, PC) in the SML was determined in relation to the sum of the concentrations of the individual lipid classes (PE, PG, PC) in the ULW and is called EF_{SML} of phospholipids ($EF_{SML(PP)}$) in the following

GL* - Glycolipids, including MGDG, DGDG, SQDG. The same calculation as for PP applies, except that the individual lipid classes MGDG, DGDG, SQDG were considered for the glycolipids and are referred to as EF_{SML} of glycolipids ($EF_{SML(GL)}$)

Table S7: Estimation of the surfactant activity of the individual lipid classes based on the parameter density, XLogP3-AA and topological polar surface area; NA – not available

Standards	Lipid class	Density	XLogP3-AA*	Topological Polar Surface Area/Å2
2-nonadecane	HC	0.7774	9.9	0
cetyl alcohol	ALC	0.8187	7.3	20.2
stearyl palmitate	WE	0.935	16.3	26.3
methyl palmitate	ME	NA	7.9	26.3
stearic acid	FFA	0.86	7.4	37.3
cholesterol	ST	1.067	7.5	37.3
1-stearoyl glycol	MG	0.894-0.906	7.2	66.8
glyceryl 1, 3 distearate	1,3 DG	0.894-0.906	16.2	72.8
D, L-α,β distearin	1,2 DG	0.894-0.906	16.2	72.8
tristearin	TG	0.8559	25.2	78.9
chlorophyll-*a*	PIG	NA	NA	96.4
phosphatydilgycerol	PG	NA	-2	107
L- α phosphatidylcholine	PC	NA	13.8	111
phosphatidylethanolamine	PE	1.0±0.1	6.93	139
sulfoquinovosyldiacylglycerol	SQDG	NA	10	195
galactosyldiglyceride	MGDG	NA	-3.5	203
digalactosyldiglyceride	DGDG	NA	-3.8	208

* The calculation of the octanol-water partition coefficient (K_{OW}) is based on the XLOGP3-AA method, which predicts the log K_{OW} as XLogP3-AA value of compound by using the known log K_{OW} of a reference compound as a starting point

Surfactant activity of investigated individual lipid classes:

To estimate the surface activity of the individual lipid classes based on their physicochemical properties, individual parameters, namely the density, the partitioning coefficient between octanol and water (log K_{OW}) and the topological polar surface area were considered. One physical parameter which shows a superficial correlation with bubble and/or current-transport susceptibility is specific gravity, also called relative density. An inverse relationship of this function with increased rates of surface accumulation by current seems logical since substances with lower densities would probably resist remixing into the water column once they have dissolved and concentrated at the air-water interface (Brown et al., 1992). Based on available density data from the literature presented within Table S7, we may roughly estimate that more nonpolar lipids such as FFA and ALC should have higher susceptibility for the air-water surface (surface accumulation) in comparison to GL and PP. In fact, FFA and ALC have lower molecular masses and densities compared to GL and PP. The octanol-water partition ratio, in turn, is the most common way of expressing the lipophilicity of compounds in logarithmic form. Referred to as log K_{OW} or log

P it is obtained either through experimental procedures (Rothwell et al., 2005) or prediction approaches (Mannhold et al., 2009). In general, the positive values for log K_{OW} indicate some hydrophobic character, whereas larger values lead to an increased hydrophobicity. Molecules with low or negative values for K_{OW}, however, are often defined as polar, although no direct link between K_{OW} and the charge distribution in the molecule exists. Based on ranking of XLogP3-AA data presented in Table S7, the most hydrophobic lipid would be TG. Another important factor which affects the adsorption is the solubility. According to Lundelius' rule (Lundelius, 1920), the extent of adsorption of surfactant could be assumed to be inversely proportional to its solubility in the water. An increase of polar moiety contribution in a molecule heightens its hydrophilicity which leads to an enhanced solubility in water. As the topological polar surface area (TPSA) of a molecule is defined as the surface sum over all polar atoms or molecules, primarily oxygen and nitrogen, also including their attached hydrogen atoms, it can serve as suitable measure to get a rough estimate of the magnitude of the surfactant activity of investigated lipids as illustrated in Table S5. It becomes apparent that the lower the TSPA, higher is the surfactant activity. Consequently, the hogher polar surface area of GL and PP shows a larger hydrophilicity in comparison with FFA and ALC. Since PP is indeed more soluble than FFA or ALC, we expect less surface activity.

Table S8: Enrichment factor in aerosol particles (EF_{aer}) of total lipids (∑lipids) of individual sampling days with corresponding SML and PM_1 aerosol particles samples (CVAO) and as an average

	total lipid concentration in SML		atmospheric concentration on PM_1 aerosol particles		$EF_{aer(\sum lipids)}$[1]	
date	dissolved	particulate	total lipids	sodium	dissolved[2]	particulate[3]
	µg L^{-1}		ng m^{-3}			
20/09/2017	121.5	118.1	133.6	150.6	9E+04	9E+04
25/09/2017	75.5	110.1	182.1	110.5	3E+05	2E+05
27/09/2017	55.7	61.0	173.1	52.9	7E+05	7E+05
6/10/2017	99.7	114.9	94.0	103.8	1E+05	1E+05
7/10/2017	78.6	81.6	97.7	109.8	1E+05	1E+05
10/10/2017	65.2	84.4	75.2	79.5	2E+05	1E+05
averaged	82.7	95.0	126.0	101.2	3E+05	2E+05

[1]For the calculation of $EF_{aer(\sum lipids)}$, Eq. (3) was used. For the analysis of sodium in the SML n=5 samples were investigated. In the SML the sodium concentration was 12.53 ± 0.53 g L^{-1}. Due to small relative standard deviation (4.2 % for SML), the mean value of sodium concentration in SML samples (12.53 g L^{-1}) was used for the calculation of EF_{aer}.

[2] $EF_{aer(\sum lipids)\ dissolved}$ is based on the total lipid concentration in the dissolved fraction of the SML and the atmospheric concentration of total lipids and of sodium on PM_1 aerosol particles.

[3] $EF_{aer(\sum lipids)\ particulate}$ is based on the total lipid concentration in the particulate fraction of the SML and the atmospheric concentration of total lipids and of sodium on PM_1 aerosol particles.

Considering the sample preparation, the averaged $EF_{aer(\sum lipids)\ dissolved}$ ($3 \cdot 10^5$) is considered in the following, since the filtration (sample preparation, section 2.2.1) the particles in the dissolved fraction of seawater samples (≤0.7 µm) are in the size-range of PM_1 aerosol particles (≤1 µm). The particulate fraction in seawater covers the particle size-range 0.7-200 µm. The averaged $EF_{aer(\sum lipids)\ particulate}$ with $2 \cdot 10^5$ is similar to the $EF_{aer(\sum lipids)\ dissolved}$ ($3 \cdot 10^5$).

Table S9: Enrichment factor in aerosol particles (EF_{aer}) of the individual lipid classes along the campaign and as an average

Lipid classes	20/09/2017	25/09/2017	27/09/2017	06/10/2017	07/10/2017	10/10/2017	averaged
HC	6E+04	4E+05	4E+05	5E+05	1E+05	3E+05	3E+05
TG	7E+05	2E+06	1E+07	2E+05	1E+06	1E+06	3E+06
FFA	1E+05	3E+05	6E+05	9E+04	2E+05	1E+05	2E+05
ALC	1E+05	7E+05	4E+06	8E+05	7E+05	3E+06	1E+06
ST	8E+04	6E+05	8E+05	2E+05	5E+05	1E+06	5E+05
1,2 DG	1E+05	8E+05	1E+05	3E+05	8E+05	NA	4E+05
MG	3E+04	NA	NA	NA	NA	NA	NA
MGDG	1E+04	5E+04	1E+05	1E+04	1E+04	2E+04	4E+04
DGDG	5E+05	4E+05	1E+06	7E+02	6E+02	NA	4E+05
SQDG	3E+05	8E+05	NA	2E+05	6E+05	5E+05	5E+05
PE	2E+05	6E+04	4E+05	8E+04	8E+04	8E+04	1E+05
PG	NA	NA	1E+06	NA	1E+04	6E+03	5E+05
total lipids	9E+04	3E+05	7E+05	1E+05	1E+05	2E+05	3E+05
PP*	2E+05	6E+04	9E+05	8E+04	4E+04	4E+04	2E+05
GL**	3E+05	4E+05	7E+05	6E+04	2E+05	2E+05	3E+05

For the calculation of $EF_{aer,}$ Eq. (3) was used. For the analysis of sodium in the SML n=5 samples were investigated. In the SML the sodium concentration was 12.53 ± 0.53 g L^{-1}. Due to small relative standard deviation (4.2 % for SML), the mean value of sodium concentration in SML samples (12.53 g L^{-1}) was used for the calculation of $EF_{aer.}$ For the sodium concentration on PM_1 aerosol particles the measured atmospheric concentration, listed in Table S8, were used. Moreover, for $c\ (analyte)_{SML}$ in Eq. (3) the measured concentration of the respective lipid class of the dissolved fraction in the SML was used for the calculation as shown in Table S8.

PP* - Phospholipids, including PE, PG and PC

GL* - Glycolipids, including MGDG, DGDG, SQDG

Table S10: Calculation of the adsorption coefficient in water (K_{aq}) and in air (K_a) of the individual lipid classes based on the saturation vapor pressure p and the Henry's law constants (H)

lipid classes	standard	saturation vapor pressure[1] (p)	Henry's law constants (H)	adsorption coefficient in water[2] (K_{aq})	adsorption coefficient in air[3] (K_a)
		Pa	mol m^{-3} Pa^{-1}	m^{-1}	m^{-1}
HC	2-nonadecane	6.1E-02	1.45E-07[a]	8.17E+03	2.94E+00
WE	stearyl palmitate	1.74E-09	8.62E-06[a]	1.50E+08	3.21E+06
ME	methyl palmitate	2.82E-02	1.80E-03[b]	6.15E-02	2.74E-01
TG	tristearine	1.3175E-21	7.00E-03[c]	2.96E+17	5.14E+18
FFA	stearic acid	4.99E-05	8.40E-01[b]	9.64E-01	2.01E+03
ALC	cetyl alcohol	7.49E-03	3.90E-02[b]	1.81E-02	1.75E+00
ST	cholesterol	1.024E-07	5.80E-02[c]	4.79E+02	6.88E+04
MG	1,2-octadecanediol	6.99E-06	8.13E-01[a]	1.75E-01	3.52E+02
PG	phosphatidylglycerol	9.94E-17	1.92E+11[a]	5.43E-01	2.59E+14
PC	L- α phosphatidylcholine	9.05E-15	6.17E+16[a]	6.20E-10	9.4916E+10
1,2 DG	diacyl-glycerol	5.69E-15	4.24E+01[a]	2.51E+06	2.6409E+11
1,3 DG	glyceryl 1, 3 distearate	5.69E-15	4.24E+01[a]	3.27E+05	3.4391E+10
DGDG	digalactosyl diglyceride	1.53E-22	5.18E+19[a]	1.03E-03	1.3251E+20
MGDG	monogalactosyldiglyceride	7.34E-18	8.62E+13[a]	2.98E-02	6.3667E+15
SQDG	sulfoquinovosyldiacylglycerol	7.46E-24	2.98E+15[a]	2.10E+02	1.5497E+21
PE	phosphatidylethanolamine	5.02E-14	2.64E+16[a]	1.50E-08	9.7974E+11

[1] saturation vapor pressure at 298.15 K was calculated with SIMPOL.1 (Pankow and Asher, 2008)

[a] Henry's Law Constants at 298.15 K was calculated by HENRYWIN by US EPA. [2011]. Estimation Programs Interface Suite™ for Microsoft® Windows, v 3.20. United States Environmental Protection Agency, Washington, DC, USA.

[b] Henry's Law Constants was calculated by Hilal et al. (2008) as mentioned in Sander (2015)

[c] Henry's Law Constants was calculated based on the method by Meylan and Howard (1991) as mentioned in Sander (2015)

[2] The adsorption coefficient in water (K_{aq}) was calculated using equation (4):

$$K_{aq} = \frac{\frac{c(analyte)_{SML}}{1 \cdot 10^{-6}}}{H_{A(analyte)} \cdot p_{analyte}} \quad (4)$$

with $c(analyte)_{SML}$ as mean concentration of the analyte in the dissolved fraction of the SML (in mol m^{-3}), the mean thickness of SML ($1 \cdot 10^{-6}\, m$), the Henry's law constants of the analyte $H_{A(analyte)}$ (in mol m^{-3} Pa^{-1}) and $p_{analyte}$ (saturation vapor pressure at 298.15 K in Pa).

[3] The adsorption coefficient in air (K_a) was calculated using equation (5):

$$K_a = \frac{\frac{c(analyte)_{SML}}{1 \cdot 10^{-6}}}{\frac{p_{analyte}}{R \cdot T}} \quad (5)$$

with $c(analyte)_{SML}$ as mean concentration of the analyte in the dissolved fraction of the SML (in mol m^{-3}), the mean thickness of SML ($1 \cdot 10^{-6}\, m$), $p_{analyte}$ (saturation vapor pressure at 298.15 K in Pa=N m^{-2}= kg m^{-1} s^{-2}), the gas constant R (8.314 kg m^2 s^{-2} mol^{-1} K^{-1}) and the temperature T (298.15 K).

Adsorption of the individual lipid classes at bubble air-water interface:

To estimate the adsorption of the individual lipid classes at the air-water interface, both the adsorption coefficient in water (K_{aq}) and the one in air (K_a) were calculated, as shown in Table S10. Considering the concentration of the adsorbed solute at the air-water interface as well as the equilibrium concentration of the solute, the principle of K_a was based on the approach of Kelly et al. (2004). According to it, the concentration in the SML and the saturation vapor pressure (p) of the analyte describe the distribution of the analyte between the interface and the air, namely K_a. Also, another new adsorption coefficient, K_{aq}, was introduced in this context. It takes into account the concentration of the adsorbed solute at the air-water interface, but uses the saturation concentration of the solute in water instead of air. The saturation concentration of the solute in water was calculated by multiplying p with the Henry's Law (H_A) constant of the analyte. As for most analytes no H_A constants has been determined, however, which is also the case for p, estimation programs had been applied to calculate these values. Table S10 shows how. The parameters p and H_A for the standards of the individual lipid classes were calculated. A comparison of p by using different models (SIMPOL.1 vs. EVAPORATION) is further discussed in Fig. S18.

Overall, the results in Table S10 help evaluating the possible adsorption of the individual lipid classes at the bubble air-water interface could be evaluated. Assuming that the differences between both adsorption coefficients, K_{aq} and K_a, were between 10^1 and 10^2, K_{aq}~K_a was defined. For example, this applied to TG with $K_{aq(TG)}$:$2.96 \cdot 10^{17}$, $K_{a(TG)}$:$5.14 \cdot 10^{18}$ and ALC with $K_{aq(ALC)}$:$1.81 \cdot 10^{-2}$, $K_{a(ALC)}$:$1.75 \cdot 10^{0}$. Based on the ratio of the two adsorption coefficients to each other (K_{aq}~ K_a), we conclude that the lipid classes TG and ALC are preferably distributed at the interface, the bubble surface. As regards the EF_{aer} (Table S9), TG and ALC showed the comparatively highest EF_{aer} with $3 \cdot 10^6$ and with $1 \cdot 10^6$, respectively. In contrast, if we look at the lipid class which had the comparatively lowest EF_{aer} ($4 \cdot 10^4$), the ratio of the adsorption coefficients was K_a>>K_{aq} for MGDG, meaning that it was preferably distributed into water.

References

Brown, J. W., Skop, R. A., Viechnicki, J., and Tseng, R.-S.: Transport of surface-active organic materials from seawater to the air-water interface by an ascending current field, Fluid Dynamics Research, 9, 97-105, 1992.

Compernolle, S., Ceulemans, K., and Müller, J. F.: EVAPORATION: a new vapour pressure estimation methodfor organic molecules including non-additivity and intramolecular interactions, Atmos. Chem. Phys., 11, 9431-9450, 10.5194/acp-11-9431-2011, 2011.

Duhamel, S., Kim, E., Sprung, B., and Anderson, O. R.: Small pigmented eukaryotes play a major role in carbon cycling in the P-depleted western subtropical North Atlantic, which may be supported by mixotrophy, Limnol. Oceanogr., 64, 2424-2440, 10.1002/lno.11193, 2019.

Hilal, S. H., Ayyampalayam, S. N., and Carreira, L. A.: Air−Liquid Partition Coefficient for a Diverse Set of Organic Compounds: Henry's Law Constant in Water and Hexadecane, Environ. Sci. Technol., 42, 9231-9236, 10.1021/es8005783, 2008.

Kelly, C. P., Cramer, C. J., and Truhlar, D. G.: Predicting Adsorption Coefficients at Air−Water Interfaces Using Universal Solvation and Surface Area Models, The Journal of Physical Chemistry B, 108, 12882-12897, 10.1021/jp037210t, 2004.

Lundelius, E. F.: Adsorption and solubility, Kolloid-Z. , 26, 145-151, 1920.

Mannhold, R., Poda, G. I., Ostermann, C., and Tetko, I. V.: Calculation of Molecular Lipophilicity: State-of-the-Art and Comparison of LogP Methods on more than 96,000 Compounds, Journal of Pharmaceutical Sciences, 98, 861-893, 10.1002/jps.21494, 2009.

Meylan, W. M., and Howard, P. H.: Bond contribution method for estimating henry's law constants, Environmental Toxicology and Chemistry, 10, 1283-1293, 10.1002/etc.5620101007, 1991.

Pankow, J. F., and Asher, W. E.: SIMPOL.1: a simple group contribution method for predicting vapor pressures and enthalpies of vaporization of multifunctional organic compounds, Atmos. Chem. Phys., 8, 2773-2796, 10.5194/acp-8-2773-2008, 2008.

Rothwell, J. A., Day, A. J., and Morgan, M. R. A.: Experimental Determination of Octanol−Water Partition Coefficients of Quercetin and Related Flavonoids, Journal of Agricultural and Food Chemistry, 53, 4355-4360, 10.1021/jf0483669, 2005.

Sander, R.: Compilation of Henry's law constants (version 4.0) for water as solvent, Atmos. Chem. Phys., 15, 4399-4981, 10.5194/acp-15-4399-2015, 2015.

Zäncker, B., Cunliffe, M., and Engel, A.: Bacterial Community Composition in the Sea Surface Microlayer Off the Peruvian Coast, Front Microbiol, 9, 2699-2699, 10.3389/fmicb.2018.02699, 2018.